

Interaction and excitonic insulating transition in graphene

Guo-Zhu Liu, Wei Li, and Geng Cheng

Department of Modern Physics, University of Science and Technology of China, Hefei, Anhui, 230026, P.R. China

The strong long-range Coulomb interaction between massless Dirac fermions in graphene can drive a semimetal-insulator transition. We show that this transition is strongly suppressed when the Coulomb interaction is screened by such effects as disorder, thermal fluctuation, doping, and finite volume. It is completely suppressed once the screening factor μ is beyond a threshold μ_c even for infinitely strong coupling. However, such transition is still possible if there is an additional strong contact four-fermion interaction. The differences between screened and contact interactions are also discussed.

PACS numbers: 73.43.Nq, 71.10.Hf, 71.30.+h

The low-energy elementary excitations in undoped graphene are massless Dirac fermions. Their spectral and transport properties are quite unusual and have attracted intense investigations in the past several years [1, 2]. For a clean undoped graphene, the density of states (DOS) $N(\omega)$ vanishes linearly near the Dirac point. As a result, the Coulomb interaction between massless Dirac fermions is essentially unscreened, in sharp contrast to the electron system with parabolic dispersion. The unscreened, long-range Coulomb interaction was shown to be responsible for many anomalous behaviors of graphene [3, 4, 5, 6, 7].

At the strong coupling regime, the long-range Coulomb interaction can open a finite mass gap for the Dirac fermion, which then drives a phase transition from the semimetal state to an insulator state. This transition is realized by forming stable particle-hole pairs and usually named as excitonic semimetal-insulator (SM-IN) transition [4, 5]. Recently, this kind of phase transition has been studied by nonperturbative Dyson-Schwinger (DS) equation approach [4, 5], renormalization group method [7], and lattice simulation [8]. The SM-IN transition was found in graphene for strong Coulomb coupling and small fermion flavor [4]. The effects of finite temperature and external magnetic field were also considered [5].

Although being of remarkable interests, the predicted SM-IN transition (in zero magnetic field) has not yet been unambiguously observed in experiments. In this paper, we discuss the effects that can potentially prevent the appearance of this SM-IN transition. First of all, it should be emphasized that such transition can take place only for strong, poorly screened Coulomb interaction. Generically, there are two critical parameters: critical dimensionless coupling strength λ_c and critical fermion flavor N_c . SM-SI transition is possible only when $N < N_c$ and $\lambda > \lambda_c$. Once the long-range Coulomb interaction is screened by some physical effects, there will be an effective screening factor μ , which is expected to increase λ_c and reduce N_c . This can be understood by noting the important fact that SM-SI transition realized by forming fermion-antifermion pairs is a genuine low-energy phenomenon. From the experience in QED₃, the long-range nature of gauge interaction plays the crucial role in generating the dynamical mass gap for initially

massless Dirac fermions [9]. A finite gauge boson mass rapidly reduces the critical fermion flavor to below the physical value 2 [9]. In the present case, there is a similar suppressing effect once the long-range Coulomb interaction is screened. The opening of an excitonic gap requires the Coulomb interaction sufficiently strong at low-momentum region. However, the screening factor μ suppresses the contribution from small momenta significantly. Obviously, this kind of pairing instability is markedly different from the conventional BCS-type pairing formation, which is caused by arbitrary weak attractive force between electrons.

In realistic graphene samples, the critical behavior of SM-IN transition can be influenced by the following reasons: disorder; thermal fluctuation; doping; finite sample volume. Each of them can generate an effective screening factor μ , which could be regarded as an effective photon mass. We study their effects on critical strength λ_c and critical flavor N_c by solving the corresponding gap equation, and show that a growing μ significantly increases λ_c and reduces N_c , both at zero and finite temperatures. When μ is beyond some threshold μ_c , the excitonic transition is completely suppressed, leaving semi-metal as the stable ground state. Frequently, some of these effects coexist in reality, leading to further suppression of SM-IN transition. We also discuss the difference between screened Coulomb interaction and contact interaction. After including a contact four-fermion interaction to the system, we found that it can drive the system towards an SM-IN transition when its coupling is strong enough.

The total Hamiltonian of massless Dirac fermion $H = H_0 + H_C$ is given by

$$H_0 = v_F \sum_{\sigma=1}^N \int_{\mathbf{r}} \bar{\psi}_{\sigma}(\mathbf{r}) i\boldsymbol{\gamma} \cdot \nabla \psi_{\sigma}(\mathbf{r}),$$
$$H_C = \frac{1}{4\pi} \sum_{\sigma, \sigma'}^N \int_{\mathbf{r}, \mathbf{r}'} \bar{\psi}_{\sigma}(\mathbf{r}) \gamma_0 \psi_{\sigma}(\mathbf{r}) \frac{e^2}{|\mathbf{r} - \mathbf{r}'|} \bar{\psi}_{\sigma'}(\mathbf{r}') \gamma_0 \psi_{\sigma'}(\mathbf{r}').$$

Here, we adopt four-component spinor field ψ to describe the massless Dirac fermion since there is no chiral symmetry in the two-component representation. The conjugate spinor field is defined as $\bar{\psi} = \psi^{\dagger} \gamma_0$. The 4×4 γ -matrices

satisfy the standard Clifford algebra. Although the physical fermion flavor is actually $N = 2$, in the following we consider a large N in order to perform $1/N$ expansion. The total Hamiltonian preserves a continuous $U(2N)$ chiral symmetry $\psi \rightarrow e^{i\theta\gamma_5}\psi$, which will be dynamically broken if a nonzero fermion mass gap is generated.

The free propagator of massless Dirac fermion is $G_0(k_0, \mathbf{k}) = (\gamma_0 k_0 - v_F \boldsymbol{\gamma} \cdot \mathbf{k})^{-1}$. The Coulomb interaction modifies it to the complete propagator

$$G^{-1}(k_0, \mathbf{k}) = \gamma_0 k_0 A_1(k) - v_F \boldsymbol{\gamma} \cdot \mathbf{k} A_2(k) - m(k), \quad (1)$$

where $m(k)$ denotes the dynamical fermion mass and $A_{1,2}$ the wave function renormalization functions. To the leading order in $1/N$ expansion, the DS integral equation is

$$G^{-1}(p) = G_0^{-1}(p) + \int \frac{d^3k}{(2\pi)^3} \gamma_0 G(k) \gamma_0 V(p-k), \quad (2)$$

where the vertex function has already been approximated by the bare matrix γ_0 . The nontrivial solution $m(p)$ of this equation signals the opening of an excitonic gap.

In the DS gap equation, $V(q)$ is the Coulomb interaction function. The bare, unscreened Coulomb interaction has the form $V_0(q) = \frac{g_C^2}{2|\mathbf{q}|}$ in the momentum space. For an interacting electron gas, the collective density fluctuations screen the bare Coulomb interaction $V_0(q)$ to $V^{-1}(q) = V_0^{-1}(q) - \pi(q)$. For ordinary non-relativistic electron gas, the static polarization function $\pi(q_0 = 0)$ is just the zero-energy DOS, $N(0)$, which is known to be finite. The parameter $N(0)$ defines the inverse Thomas-Fermi screening length. The case for undoped clean graphene is quite different because of the linear dispersion of Dirac fermions. The leading contribution to polarization function is given by

$$\pi_0(q) = -\frac{N}{8} \frac{\mathbf{q}^2}{\sqrt{q_0^2 + v_F^2 |\mathbf{q}|^2}}. \quad (3)$$

It vanishes linearly as $\mathbf{q} \rightarrow 0$ in the static limit $q_0 = 0$, so the long-range Coulomb interaction is unscreened.

Under the approximations described above, the gap equation can be written as

$$m(p^2) = \frac{1}{N} \int \frac{dk_0}{2\pi} \int \frac{d^2\mathbf{k}}{(2\pi)^2} \frac{m(k^2)}{k_0^2 + |\mathbf{k}|^2 + m^2(k^2)} \times \frac{1}{\frac{|\mathbf{p}-\mathbf{k}|}{8\lambda} + \frac{1}{8} \frac{|\mathbf{p}-\mathbf{k}|^2}{\sqrt{(p_0-k_0)^2 + |\mathbf{p}-\mathbf{k}|^2}}}, \quad (4)$$

where $A_{1,2} = 1$ is assumed and the scaling $v_F \mathbf{k} \rightarrow \mathbf{k}$, $v_F \Lambda \rightarrow \Lambda$ is made. The present problem contains two parameters: fermion flavor N and dimensionless Coulomb coupling defined as $\lambda = g_C^2 N / 16 v_F$, where $g_C = e^2 / \epsilon_0$. The ultraviolet cutoff Λ is taken to be of order 10eV which is determined by $\sim a^{-1}$ with lattice constant $a = 2.46 \text{ \AA}$. Not that no instantaneous approximation for the polarization function is made at present. We solve the nonlinear gap equation using bifurcation theory and

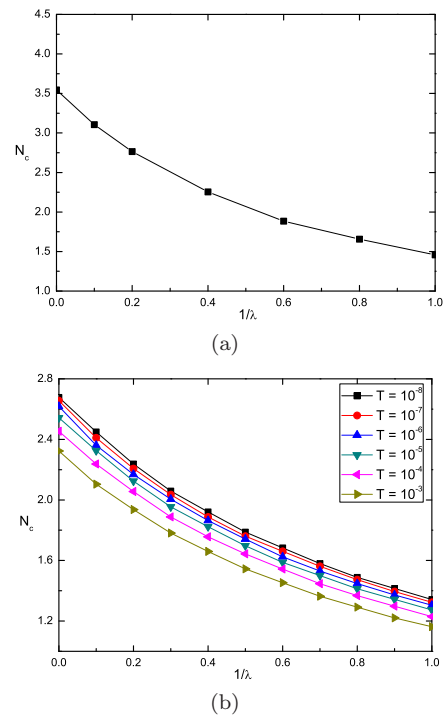


FIG. 1: (a) Relationship between N_c and λ at zero temperature; (b) Relationship between N_c and λ at different temperatures T . Both are for unscreened Coulomb interaction.

parameter embedding method [9, 10] for a number of fixed values of λ . The fermion flavor N serves as the embedded parameter in seeking the bifurcation point. The results are shown in Fig. 1(a). It is easy to see that the critical flavor N_c is an increasing function of λ . For $\lambda \rightarrow \infty$, $N_c \approx 3.52$; for $\lambda = 2$, $N_c \approx 2$.

The above results are valid only for the unscreened Coulomb interaction at zero temperature. In realistic systems, the long-range interaction can be screened by several physical effects. Rather than calculating the polarization function by taking each effect into account, we phenomenologically introduce a single screening factor μ (in unit of eV) to the interaction function

$$V(q) = \frac{1}{\frac{|\mathbf{q}|}{8\lambda} + \frac{1}{8} \frac{|\mathbf{q}|^2}{\sqrt{q_0^2 + |\mathbf{q}|^2}} + \mu}, \quad (5)$$

and then discuss these effects separately. The advantage of this form is that it explicitly measures the suppressing effect on the critical behavior due to all possible screening mechanisms. If we regard this function as the effective interaction strength, then the influence of μ becomes clear: it eliminates the contribution of small momenta to the gap equation (4). But remember that the excitonic gap generation is primarily determined by the contribution from this region, so it is expected that a large μ will destroy SM-IN transition. By straightforward computation of the gap equation, we found that a growing μ leads to increase of critical strength λ_c and to decrease of critical

flavor N_c (see Fig. 2(a)). Beyond some critical value μ_c , the SM-IN transition is completely prevented, even when the dimensionless strength $\lambda \rightarrow \infty$.

The possible screening mechanisms will be discussed in order. First, disorders are unavoidable in graphene samples. They can be crudely classified as random mass, random chemical potential, and random vector potential, *etc.*, and have been extensively treated using various field theoretic techniques [11, 12, 13, 14, 15]. The low-energy DOS was found to be sensitive to the symmetry of disorders [13, 14, 15]. For instance, random vector potential leads the DOS to vanish algebraically upon approaching the Fermi surface with exponent depending on symmetry [13, 15]. For this kind of disorder, there is essentially no screening effect and the Coulomb interaction remains long-ranged, provided that the Altshuler-Aronov type correction to low-energy DOS is not included. For random mass potential, the zero-energy DOS can have finite value, as a result of dynamical discrete symmetry breaking [11, 14]. In the case of weak disorders, the impurity scattering can be treated within the conventional self-consistent Born approximation, which reveals that the zero-energy DOS acquires a finite value of the form [12]

$$N(0) = \frac{N}{\pi^2 v_F^2} \Gamma_0 \ln \frac{\Lambda}{\Gamma_0} \quad (6)$$

with a constant scattering rate Γ_0 . The finite $N(0)$ screens the long-range Coulomb interaction. It can be seen by including Γ_0 into polarization function. It is, however, not easy to get a form suitable for the present usage. Instead of performing explicit calculation, we simply assume that the screening factor $\mu = N(0)$. The dependence of N_c on Γ_0 for different λ is presented in Fig. 2(b), which shows that the growing scattering rate Γ_0 has the same qualitative effects as screening factor μ , i.e., it significantly reduces N_c and increases λ_c . One might argue that the low-energy fermionic excitations are all suppressed once a fermion mass gap opens, and that DOS vanishes at energy scale below the gap. However, for fermion of mass m , the zero-energy DOS was found [16] to be $N(0) = \frac{2}{\pi^2 v_F^2} \Gamma_0 \ln \frac{\Lambda}{\sqrt{\Gamma_0^2 + m^2}}$. Since the critical behavior of SM-IN transition is studied by linearizing the nonlinear gap equation, the mass can be safely set to zero near the bifurcation point. The expression (6) is recovered at the limit $m \rightarrow 0$.

Secondly, the thermal fluctuation will surely restore the chiral symmetry even it is broken by the ground state. The Matsubara fermion propagator is $\mathcal{G}(i\omega_n, \mathbf{k}) = (i\omega_n \gamma_0 - v_F \boldsymbol{\gamma} \cdot \mathbf{k} - m)^{-1}$, where $\omega_n = (2n + 1)\pi T$ is the fermion frequency. The polarization function can be approximated [17] by $\pi(0, \mathbf{q}) = \frac{e^2}{8v_F^2} (v_F \mathbf{q} + cT \exp(-\frac{v_F \mathbf{q}}{cT}))$ with constant $c = 16 \ln 2/\pi$. Here, in order to carry out the frequency summation, we utilize the instantaneous approximation [4, 5]. At the limit $\mathbf{q} \rightarrow 0$, the polarization is $\sim T$, corresponding to a thermal screening factor. Since other screening effects can coexist with thermal

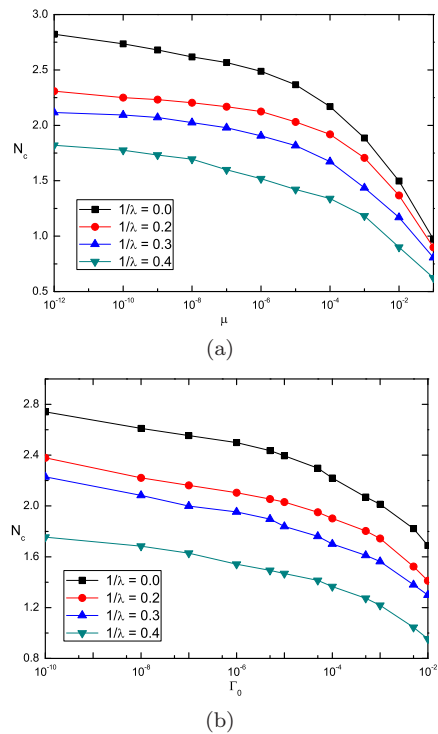


FIG. 2: (a) Dependence of N_c on μ for different values of λ ; (b) Dependence of N_c on Γ_0 for different values of λ .

fluctuations at finite temperatures, we still introduce the parameter μ and write the gap equation as

$$m(\mathbf{p}, \beta) = \frac{1}{N} \int \frac{d^2 \mathbf{k}}{8\pi^2} m(\mathbf{k}, \beta) \frac{\tanh \frac{\sqrt{\mathbf{k}^2 + m^2(\mathbf{k}, \beta)}}{2T}}{\sqrt{\mathbf{k}^2 + m^2(\mathbf{k}, \beta)}} \times \frac{1}{\frac{|\mathbf{p}-\mathbf{k}|}{16\lambda} + \frac{1}{8} (|\mathbf{p}-\mathbf{k}| + cT e^{-\frac{|\mathbf{p}-\mathbf{k}|}{cT}}) + \mu}.$$

The results at finite temperatures are rather complex since now we have four parameters, N , λ , T , μ , each of which has a critical value. Their relationships are shown in Fig. 1(b) without screening effects ($\mu = 0$) and in Fig. 3(a) with screening (the temperature is in unit of eV). In Fig. 3(a), the Coulomb coupling parameter is fixed at $\lambda \rightarrow \infty$, and the results for other values of λ are not shown since they are qualitatively similar. The results tell us that the thermal suppression is more important than screening effect when μ has small values ($< 10^{-5}$), but the screening effect eventually becomes much more important than thermal effect for larger values of μ .

The third potential mechanism that can prevent gap generation is doping. If the graphene is slightly doped, the finite carrier density then serves as the effective screening factor μ . This implies that the excitonic gap is expected to open only at or very close to the Dirac point. The critical carrier density has been discussed previously by Gorbar *et al.* [5]. Recently, the same screening effect was emphasized when studying the exciton condensate in bilayer graphene. In particular, it was found [18] that

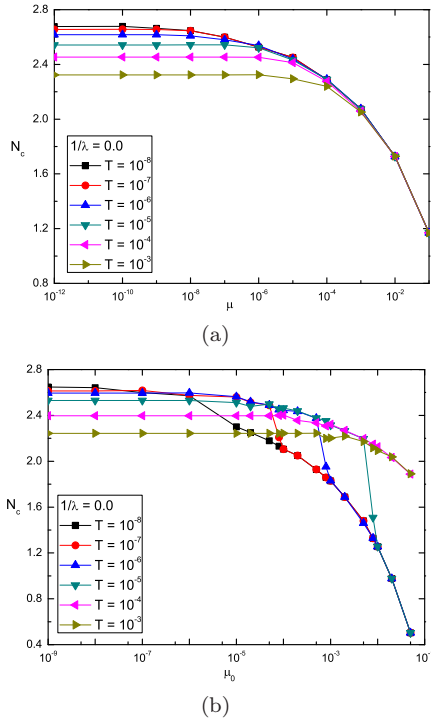


FIG. 3: (a) Dependence of N_c on μ for different T at $\lambda \rightarrow \infty$; (b) Dependence of N_c on μ_0 for different T at $\lambda \rightarrow \infty$.

the screening suppress the mean-field pairing temperature by a factor of 10^{-7} . We solved the gap equation after incorporating the polarization function [5] that contains temperature T and chemical potential μ_0 , and show the results in Fig. 3(b) (also at $\lambda \rightarrow \infty$ for comparison). The dependence of N_c on T and μ_0 qualitatively resembles that in Fig. 3(a), but visibly exhibits different quantitative behavior: the suppressing effect from doping is more prominent at low T than at higher T . Despite the details, a large doping makes the excitonic insulating state impossible.

Finally, we discuss effect of finite sample volume (area in two dimensions). For a graphene plane of finite spatial extent, the particle momenta becomes discrete and the momenta transferred in the process of interaction can not be arbitrary small. If we still work in the continuum field theoretic formalism, this effect can be equivalently represented by imposing an infrared cutoff κ , given by the inverse sample size L^{-1} . Its effects on N_c is nearly the same as Fig. 2(a) at $T = 0$ and Fig. 3(a) at finite T with μ replaced by κ , and hence are not presented explicitly. The results imply that the sample of large spatial extension is more favorable to undergo the SM-IN transition [19].

Besides the effects discussed above, any mechanism that can screen the long-range Coulomb interaction will also unavoidably lower the possibility of gap generation. If more than one screening effects coexist in reality, the suppression of SM-IN transition becomes more significant, as shown in Fig. 2(a) and 3(a). In light of these re-

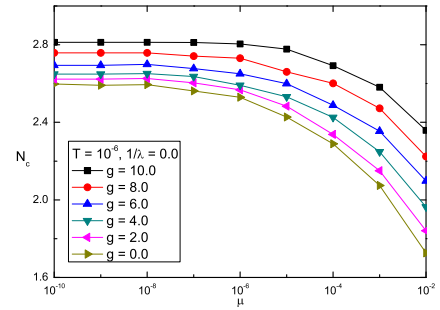


FIG. 4: Dependence of N_c on μ for different g .

sults, we conclude that the excitonic insulating state can most probably be observed in undoped, clean graphene of large area near absolutely zero temperature.

Once the long-range Coulomb interaction is screened, one interesting question is whether it can be equivalently replaced by a short-range or even a contact (on-site) repulsive interaction [2]. This question can also be asked in another way: is the long-range nature or the strong coupling nature of Coulomb interaction more important in driving the SM-IN transition? If the answer is the latter, then the long-range interaction can well be replaced by a short-range or contact one. According to our results, it seems that the long-range, rather than strong coupling, nature plays the dominant role. As shown in Fig. 2(a), even in the very strong coupling limit $\lambda \rightarrow \infty$, the critical flavor N_c is already less than the physical flavor 2 when the screening factor $\mu \sim 10^{-3}$. For moderately strong coupling $\lambda = 2.5$, the excitonic insulating behavior becomes impossible even if the screening factor is only as small as $\mu \sim 10^{-12}$.

In order to test the role of contact interaction and see its difference from the screened Coulomb interaction, we add one quartic interacting term to the Hamiltonian. There are several choices for the four-fermion coupling term, classified by the gamma matrices used to define the action [20, 21]. For simplicity, we consider only one of them, i.e.,

$$\frac{G}{N} \sum_{\sigma} \int_{\mathbf{r}} (\bar{\psi}_{\sigma}(\mathbf{r}) \psi_{\sigma}(\mathbf{r}))^2. \quad (7)$$

To the lowest order, this contact interaction contributes the following term to the gap equation

$$\frac{g}{N\Lambda} \int \frac{d^2\mathbf{k}}{8\pi^2} \frac{m(\mathbf{k}, \beta) \tanh \frac{\sqrt{\mathbf{k}^2 + m^2(\mathbf{k}, \beta)}}{2T}}{\sqrt{\mathbf{k}^2 + m^2(\mathbf{k}, \beta)}}, \quad (8)$$

where the dimensionless coupling is $g = NGA/v_F$ and the scaling $v_F \mathbf{k} \rightarrow \mathbf{k}$, $v_F \Lambda \rightarrow \Lambda$ is made as before. The whole gap equation is solved with results shown in Fig. 3(b) at $T = 10^{-6}$ eV (~ 10 mK). The contact four-fermion interaction has opposite effect on the critical flavor N_c as compared with the screening factor μ : while the latter rapidly suppresses N_c , the former is very efficient in promoting the system towards the excitonic insulating phase

(note there is no Goldstone boson in the insulating phase since now the total Hamiltonian preserves discrete chiral symmetry $\psi \rightarrow \gamma_5 \psi$, rather than continuous one). Thus we see that the contact four-fermion interaction is actually different from screened Coulomb interaction. For a relatively large screening factor μ , the latter is unable to generate excitonic gap even in the $\lambda \rightarrow \infty$ limit, while the former can generate such gap when its coupling is larger than some critical value $g > g_c$. The reason for this can be seen from the gap equation: for the Coulomb interaction part, \mathbf{q} appeared in the denominator suppresses the

contribution from large momenta and μ in the denominator suppresses the contribution from small momenta; on the contrary, for contact fermion interaction, the coupling g is constant in the whole momenta region without any suppressing effect. In conclusion, the SM-IN transition is still possible if there is additional strong contact fermion interaction, even when the screened Coulomb interaction itself is unable to open the gap.

The work was supported by the National Science Foundation of China under Grant No. 10674122.

-
- [1] A. K. Geim and K. S. Novoselov, *Nat. Mater.* **6**, 183 (2007).
- [2] A. H. Castro Neto, F. Guinea, N. M. R. Peres, K. S. Novoselov, and A. K. Geim, *Rev. Mod. Phys.* (2008).
- [3] J. Gonzalez, F. Guinea, and M. A. H. Vozmediano, *Nucl. Phys. B* **424**, 595 (1994); *Phys. Rev. Lett.* **77**, 3589 (1996); *Phys. Rev. B* **59**, R2474 (1999).
- [4] D. V. Khveshchenko, *Phys. Rev. Lett.* **87**, 246802 (2001); D. V. Khveshchenko and H. Leal, *Nucl. Phys. B* **687**, 323 (2004).
- [5] E. V. Gorbar, V. P. Gusynin, V. A. Miransky, and I. A. Shovkovy, *Phys. Rev. B* **66**, 045108 (2002).
- [6] I. F. Herbut, *Phys. Rev. Lett.* **97**, 146401 (2006); O. Vafek and M. J. Case, *Phys. Rev. B* **77**, 033410 (2008).
- [7] D. T. Son, *Phys. Rev. B* **75**, 235423 (2007).
- [8] S. J. Hands and C. G. Strouthos, arXiv:0806.4877; J. E. Drut and T. A. Lahde, arXiv:0807.0834.
- [9] G.-Z. Liu and G. Cheng, *Phys. Rev. D* **67**, 065010 (2003).
- [10] G. Cheng and T. K. Kuo, *J. Math. Phys.* **35**, 6270 (1994); **35**, 6693 (1994).
- [11] M. P. A. Fisher and E. Fradkin, *Nucl. Phys. B* **241**, 457 (1985); E. Fradkin, *Phys. Rev. B* **33**, 3263 (1986).
- [12] P. A. Lee, *Phys. Rev. Lett.* **71**, 1887 (1993); A. Durst and P. A. Lee, *Phys. Rev. B* **62**, 1270 (2000).
- [13] A. W. W. Ludwig, M. P. A. Fisher, R. Shankar, and G. Grinstein, *Phys. Rev. B* **50**, 7526 (1994).
- [14] A. A. Nersisyan, A. M. Tsvelik, and F. Wenger, *Nucl. Phys. B* **438**, 561 (1995).
- [15] A. Altland, B. D. Simons, and M. R. Zirnbauer, *Phys. Rep.* **359**, 283 (2002); F. Evers and A. D. Mirlin, *Rev. Mod. Phys.* **80**, 1355 (2008).
- [16] V. P. Gusynin and V. A. Miransky, *Eur. Phys. J. B* **37**, 363 (2004).
- [17] I. J. R. Aitchinson, N. Dorey, M. Klein-Kreisler, and N. E. Mavromatos, *Phys. Lett. B* **294**, 91 (1992).
- [18] M. Yu. Kharitonov and K. Efetov, arXiv:0808.2164. See, however, a comment by R. Bistritzer, H. Min, and J. J. Su, and A. H. MacDonald, arXiv:0810.0331.
- [19] The effect of infrared cutoff was discussed in QED₃ by V. P. Gusynin and M. Reenders, *Phys. Rev. D* **68**, 025017 (2003).
- [20] D. J. Gross and A. Neveu, *Phys. Rev. D* **10**, 3235 (1974).
- [21] B. Rosenstein, B. J. Warr, and S. H. Park, *Phys. Rep.* **205**, 59 (1991).